A mixed-metal salt comprised of metal–metal bonded dinuclear ions: structure and properties of $[Rh_2(OAc)_2(MeCN)_6][Re_2Cl_8]$

Kim R. Dunbar*, Laura E. Pence** and Julie L.C. Thomas[†]

Department of Chemistry and The Center For Fundamental Materials Research, Michigan State University, East Lansing, MI 48824 (USA)

(Received August 27, 1993; revised October 19, 1993)

Abstract

The unusual salt $[Rh_2(OAc)_2(MeCN)_6][Re_2Cl_8]$ (**1**) is produced from a methathetic reaction of the salt $[NBu_4{}^n]_2[Re_2Cl_8]$ with $[Rh_2(OAc)_2(MeCN)_6][BF_4]_2$. Crystal data for **1**: *Pccn*, $a=27.42(1)$, $b=26.736(4)$, $c=18.137(5)$ Å, $V=13.296(7)$ Å^3, $Z=16$, $D_{calc}=2.450$ g/cm^3, μ(Mo Kα)$=90.05$ cm^{-1}, $R=0.078$, $R_w=0.109$ for 483 parameters and 5229 data with $F_o{}^2>3\sigma(F_o)^2$. The new salt constitutes the only example of a structure wherein the octachlorodirhenate unit is present in three different crystallographic environments in the same unit cell. The asymmetric unit contains two independent $[Rh_2]^{2+}$ cations together with one $[Re_2Cl_8]^{2-}$ anion at full occupancy and two dirhenium anions each at half-occupancy. The synthesis, structure, key spectroscopic properties and solution behavior of **1** are presented and discussed.

Key words: Crystal structures; Rhodium complexes; Rhenium complexes; Mixed salt complexes; Dinuclear complexes

Introduction

The structural determination of numerous salts containing the anions $[Re_2X_8]^{2-}$ (X=F, Cl, Br, I) with a variety of cations have led to interesting findings [1]. In particular, the disorder exhibited by the nearly cubic Re_2 units has been correlated with changes in halide and cation identity, as well as temperature and solvent of crystallization. As part of our recent interest in the chemistry of all-inorganic salts that contain reactive binuclear cations [2], we have been exploring salts containing $[Re_2Cl_8]^{2-}$ together with a metal–metal bonded cation. Herein we report the synthesis, single crystal X-ray structure as well as the spectroscopic and solution behavior of the unusual salt $[Rh_2(O_2CCH_3)_2(MeCN)_6][Re_2Cl_8]$.

Experimental

Starting materials

The starting materials, $[Rh_2(OAc)_2(MeCN)_6][BF_4]_2$ and $[n\text{-}Bu_4N]_2[Re_2Cl_8]$ were prepared by literature methods [3, 4]. Bis(triphenylphosphoranylidene)-ammonium (ppn) chloride was purchased from Aldrich and was used as received. Solvents were freshly distilled under nitrogen from an appropriate drying agent prior to use.

Physical methods

IR spectra were measured as Nujol mulls on a Nicolet 740 FT-IR and a Perkin-Elmer 599 spectrophotometer; the latter was used to access the far-IR region. Electronic spectroscopy was carried out on a Cary 17 spectrophotometer in 1 cm pathlength quartz cells. Solid state electronic spectra of both reactants and products were measured as very fine suspensions in Nujol on glass microscope slides. Elemental analyses were performed by Galbraith Laboratories. A room temperature magnetic susceptibility measurement was carried out on a Johnson-Matthey magnetic susceptibility balance.

---

*Author to whom correspondence should be addressed.

**Present address: Department of Chemistry, Massachusetts Institute of Technology, Cambridge, MA 02140, USA.

[†] Present address: Department of Chemistry, Texas A&M University, College Station, TX 77840, USA.

SSDI 0020-1693(93)03751-U

Reaction procedures

All reactions were carried out under a nitrogen atmosphere using standard Schlenk-line techniques unless otherwise specified.

Synthesis of [$Rh_2(OAc)_2(MeCN)_6$][Re_2Cl_8] (1)

Method 1. In a typical reaction, 116 mg of [$Rh_2(OAc)_2(MeCN)_6$][BF_4]$_2$ (0.156 mmol) and 175 mg of [n-Bu_4N]$_2$[Re_2Cl_8] (0.153 mmol) were stirred in 15 ml of MeCN for 90 min. A lavender precipitate and a navy blue solution began forming within *c.* 5 min. After 30 min, the solid was allowed to settle out, and the solvent was decanted. The purple solid was washed with 4×10 ml of MeCN to remove residual [n-Bu_4N][BF_4] and dried *in vacuo*; yield 132 mg (70%). IR (CsI, Nujol), cm^{-1}: 2329(w), 2308(w), 2304(w), 2280(w), 1555(m), 1538(m), 1057(m), 1037(m), 338(s).

Method 2. A quantity of [$Rh_2(OAc)_2(MeCN)_6$][BF_4]$_2$ (116 mg, 0.156 mmol) was dissolved in 5 ml of MeCN to give a wine solution which was layered over a blue–green solution of [n-Bu_4N]$_2$[Re_2Cl_8] (175 mg, 0.153 mmol) dissolved in a mixture of MeCN (10 ml) and CH_2Cl_2 (1 ml). Slow diffusion of the two reactant solution layers afforded a crop of black microcrystalline needles in a dark blue solution; additional microcrystalline product was obtained by chilling the solution to 0 °C. The long rod-like crystals exhibited pleochroism, as they appear to be black when viewed along the long axis and colorless when viewed normal to the needle axis. The dark crystals became a pale lavender color upon crushing. The solvent was decanted and the crystals were washed with several aliquots of MeCN (10 ml) and dried *in vacuo*; yield 60 mg (32%). IR data (CsI, Nujol), cm^{-1}: 2327(m), 2311(w), 2301(w), 2279(m), 1557(s), 1538(s), 1029(m), 335(s). *Anal.* Calc. for $C_{16}H_{24}Cl_8N_6O_4Re_2Rh_2$: C, 15.67; H, 1.97; Cl, 23.13. Found: C, 15.95; H, 2.05; Cl, 24.59%.

Decomposition of [$Rh_2(OAc)_2(MeCN)_6$][Re_2Cl_8] in acetonitrile

A bulk sample of **1** (20 mg) was suspended in a minimum volume of MeCN (2–5 ml) and allowed to slowly dissolve over a period of 24 h to give an intensely colored blue solution. The solution was evaporated to produce a green glassy residue on the walls of the vessel. The green residue dissolves in MeCN and MeOH to yield blue solutions and in acetone to give a green solution. The product is slightly soluble in CH_2Cl_2 and insoluble in diethyl ether, benzene, hexanes, and toluene. Crystallization attempts from a variety of solvent mixtures did not produce pure materials. The IR spectrum of the crude product isolated by evaporation was recorded to identify major features. IR (CsI, Nujol), cm^{-1}: 2330(w), 2300(w), 1554(m), 1520(m), 1030(w), 720(m), 350(s), 320(m).

Reaction of [$Rh_2(OAc)_2(MeCN)_6$][BF_4]$_2$ with chloride ion

A quantity of [$Rh_2(OAc)_2(MeCN)_6$][BF_4]$_2$ (0.040 g, 0.054 mmol) and 0.051 g of [$(Ph_3)_2N$]Cl (ppnCl) (0.088 mmol) were stirred in 5 ml of MeCN at r.t. Within 2 min, the solution had turned opaque blue–purple. After 24 h, a flocculent green solid settled out of a pale purple solution. (UV–Vis of purple solution, $\lambda_{max}=550$ nm). The solvent was decanted, and the solid was washed with 5 ml of MeCN. (IR data for the green solid {CsI, Nujol}, cm^{-1}: 2330(w), 2300(w), 1560(s), 1020(s), 370(vw), 310(vw).) The electronic spectrum in CH_2Cl_2 displays a transition at $\lambda_{max}=610$ nm.

Control reaction of [Re_2Cl_8]$^{2-}$ with acetonitrile

A sample of [n-Bu_4N]$_2$[Re_2Cl_8] was dissolved in MeCN and stored at r.t. for one week in order to note if any decomposition had occurred. The electronic spectrum verified the presence of only the original compound ($\lambda_{max}=680$ nm).

X-ray crystallography

Data collection and reduction

A single crystal of **1** obtained by Method 2 with approximate dimensions 0.7×0.2×0.2 mm was mounted with epoxy on a glass fiber and examined on a CAD-4 diffractometer. A preliminary cell was established by centering on reflections chosen from a rotational photograph and the final cell was indexed on 25 reflections with $21<2\theta<28.3°$. Axial photographs as well as photographs of the [111] and [110] diagonals supported the choice of orthorhombic symmetry. The near tetragonal symmetry of the cell prompted us to gather unit cell parameters for several independent crystals at different temperatures, but we found no justification for transforming the cell to the higher symmetry crystal system. Intensity data were collected at -100 ± 2 °C over the range 4–45° using the ω-scan mode. Three periodically monitored standard reflections collected every hour indicated the crystal had decayed by an average of 6.7%; a decay correction was applied to account for this. A total of 9451 unique data was collected of which 5229 were observed with $F_o^2 \geqslant 3\sigma(F_o)^2$. Psi scans were applied to correct for absorption.

Structure solution and refinement

All calculations were carried out on a VAXSTATION 4000 computer using the TEXSAN software package. The positions of the rhenium and rhodium atoms were established by application of the SHELXS-86 solution program [5]. The remaining non-hydrogen atoms were located using DIRDIF [6] in the early stages and alternating least-squares cycles and difference Fourier maps in the later stages. A disorder of the Re4–Re5 metal unit became apparent early in the refinement.

The occupancies of both orientations were experimentally determined and fixed for final refinement. Although psi scans had been applied previously, the large number of heavy atoms in the structure coupled with the fact that the crystals were very thin plates resulted in severe absorption problems. To further correct for this, we applied the program, DIFABS. Unfortunately this did not entirely alleviate the problem, as 10 peaks in the final difference map were in the range 1.0–2.8 $e^-/Å^3$. Most of the peaks are ghosts of the Re atoms; attempts to model this e^- density as disordered metal units, however, did not produce chemically sensible results. Although this residual electron density and the large number of isotropic atoms in the final refinement contributed to a relatively high R factor, there are no doubts as to the contents of the unit cell. The N and O atoms in the immediate coordination sphere of the two dirhodium units did not behave well when refined anisotropically, therefore these and all the carbons were left isotropic. There were no non-positive definite atoms in the final refinement. The final full-matrix refinement involved 483 parameters and 5229 data for a data-to-parameter ratio of 10.8. The refinement converged with residuals of $R = 0.078$ and $R_w = 0.109$ and quality-of-fit = 2.64. The maximum shift/error in the last cycle was 0.05. A summary of the crystallographic data is found in Table 1. See also 'Supplementary material.'

Results and discussion

Synthesis and spectroscopy

The reaction to form **1** is a simple metathetic reaction involving the salts of the two large dinuclear metal ions depicted in Fig. 1. The insolubility of the $[Rh_2][Re_2]$ salt favors the formation of the kinetic product **1** which is easily separated from $[NBu_4^n][BF_4]$ before it decomposes to a thermodynamic product(s). Since further reaction occurs upon dissolution it is impossible to recrystallize the sample, therefore crystals were grown by slow diffusion of the reactants dissolved in separate solutions of MeCN. The relationship between crystals of **1** and the bulk powder form was established by IR spectroscopy. The IR spectrum of both sample types is an overlap of the individual spectra for the two starting materials minus the features for $[NBu_4^n]^+$ and $[BF_4]^-$ ions. The ν(Re–Cl) mode occurs at 335 cm^{-1} and the ν(OCO) mode for the cation is at 1550 cm^{-1}. The $\nu(C{\equiv}N)$ region for **1** is more complex than that of the $[BF_4]^-$ precursor, presumably due to solid-state splitting effects. The parent compound, $[Rh_2(OAc)_2(MeCN)_6][BF_4]_2$, exhibits three stretches of medium intensity between 2340 and 2277 cm^{-1} whereas **1** displays a pattern of two strong and two medium intensity features in this region.

TABLE 1. Crystal data for $[Rh_2(OAc)_2(MeCN)_6][Re_2Cl_8]$

Formula	$Rh_2C_{16}N_6O_4Re_2Cl_8$
Formula weight	1226.241
Space group	*Pccn*
Systematic absences	$0kl$: $l = 2n$ $h0l$: $l = 2n$ $hk0$: $h + k = 2n$
a (Å)	27.42(1)
b (Å)	26.736(4)
c (Å)	18.137(5)
α (°)	90
β (°)	90
γ (°)	90
V (Å^3)	13296(7)
Z	16
D_{calc} (g/cm^3)	2.450
Crystal size (mm)	0.7×0.2×0.2
μ(Mo Kα) (cm^{-1})	90.05
Data collection instrument	CAD-4
Radiation (monochromated in incident beam) (Å)	Mo Kα ($\lambda\bar{a} = 0.71073$)
Orientation reflections: no., range (2θ) (°)	25, $21 < 2\theta < 28.3$
Temperature (°C)	-100 ± 2
Scan method	ω
Data collection range, 2θ (°)	4–45
No. unique data, total with $F_o^2 > 3\sigma(F_o^2)$	9451, 5229
No. parameters refined	479
Transmission factors: max., min.	0.65–1.0
R[a]	0.078
R_w[a]	0.109
Quality-of-fit-indicator[c]	2.65
Largest shift/e.s.d., final cycle	0.01
Largest peak ($e^-/Å^3$)	2.79

[a] $R = \Sigma||F_o| - |F_c||/\Sigma|F_o|$. [b] $R_w = [\Sigma w|F_o| - |F_c|)^2/\Sigma w|F_o|^2]^{1/2}$; $w = 1/\sigma^2(|F_o|)$. [c] Quality of fit $= [\Sigma w(|F_o| - |F_c|)^2/(N_{obs} - N_{param})]^{1/2}$.

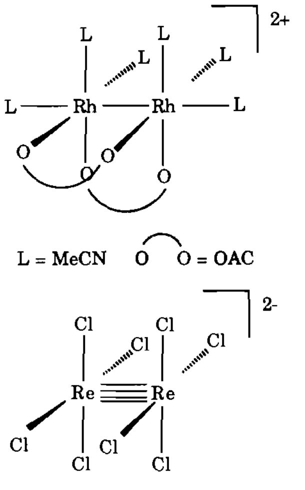

Fig. 1. Schematic drawings of the individual ions in the salt $[Rh_2(OAc)_2(MeCN)_6][Re_2Cl_8]$ (**1**).

The electronic spectrum of a dilute solution of $[Rh_2(OAc)_2(MeCN)_6][Re_2Cl_8]$ is a sum of the individual spectra for the starting materials. The main features are at $\lambda_{max} = 680$ nm, assigned to the $\delta \rightarrow \delta^*$ transition for $[Re_2Cl_8]^{2-}$, and at $\lambda_{max} = 540$ nm, attributed to the $[Rh_2(OAc)_2(MeCN)_6]^{2+}$ chromophore. Reflectance spectra on finely divided Nujol mull samples verified the presence of these two features in the solid state as well.

We were curious as to whether the salt exhibited unusual magnetic or electrical properties in addition to the optical phenomenon, thus we carried out conductivity and magnetic measurements on powder samples of **1**. Preliminary conductivity data indicated that the sample decomposed during the experiment. The compound exhibits a slight paramagnetism of 0.33 BM at r.t.; this value includes a diamagnetic correction of 20×10^{-6}/mol for Rh^{2+}, 31.5×10^{-6}/mol for acetate, 23.4×10^{-6}/mol for Cl^-, and 36×10^{-6}/mol for Re^{3+}.

Molecular structure

Selected bond distances and angles for $[Rh_2(OAc)_2(MeCN)_6][Re_2Cl_8]$ are listed in Tables 2 and 3. An ORTEP packing diagram of the unit cell is shown in Fig. 2. ORTEP plots of the individual ions are not included as they are not new molecules, and their structural features are the same as in other salts. The asymmetric unit consists of two unique dirhodium cations and three crystallographically unrelated dirhenium anions. Both of the dirhodium bis-acetate cations exhibit metric parameters similar to the original $[BF_4]^-$ salt [7]. The average Rh–Rh bond distance is 2.504(4) Å which is somewhat shorter than the analogous distance in $[Rh_2(OAc)_2(MeCN)_6][BF_4]_2$ (2.534(1) Å); presumably packing influences are responsible for this difference of ~0.03 Å. Other important distances are Rh–O = 2.01(3), Rh–N(eq) = 1.97(3) and Rh–N(ax) = 2.23(3) Å, all of which are comparable to those in the earlier structure.

TABLE 2 Table of selected bond distances (Å) for $[Rh_2(OAc)_2(MeCN)_6][Re_2Cl_8]$

Re–Re1	2.226(4)	Rh1–O4	2 01(3)
Re1–Cl1	2.31(1)	Rh1–N4	1.97(3)
Re1–Cl2	2.28(1)	Rh1–N5	1.99(3)
Re2–Re3	2.216(3)	Rh2–O1	2.03(3)
Re2–Cl5	2.31(1)	Rh2–N1	1.98(4)
Re3–Cl7	2.30(1)	Rh2–N3	2.23(3)
Re4–Re5	2.211(3)	O1–C1	1.40(4)
Re4–Cl11	2.31(1)	N1–C5	1.12(5)
Re4–Cl12	2.31(1)	N3–C9	1.12(4)
Re4A–Re5A	2.19(1)	C1–C2	1.42(6)
Re4A–Cl9	2.31(1)	Rh3–Rh4	2.498(4)
Re4A–Cl10	2.36(1)	Rh3–O6	2 03(2)
Re5–Cl10	2.31(1)	Rh3–O7	2.01(3)
Re5–Cl13	2.32(1)	Rh3–N10	2.00(3)
Re5A–Cl11	2.48(2)	Rh3–N12	2.26(4)
Re5A–Cl12	2.50(2)	Rh4–O5	2.08(3)
Rh–Rh2	2.509(4)	Rh4–N7	1.90(3)
Rh1–O2	1.99(2)	Rh4–N9	2.22(3)

TABLE 3. Table of selected bond angles (°) for $[Rh_2(OAc)_2(MeCN)_6][Re_2Cl_8]$

Re1–Re1–Cl1	104.9(3)		
Re1–Re1′–Cl2	103.2(3)		
Cl1–Re1–Cl2	86.3(4)	Cl10–Re5–Cl13	151.5(5)
Cl1–Re1–Cl3	150.4(4)	Re4A–Re5A–Cl11	96.1(6)
Cl2–Re1–Cl4	152.7(5)	Re4A–Re5A–Cl16	109.0(6)
Re3–Re2–Cl5	103.9(2)	Cl11–Re5A–Cl12	78.0(5)
Re3–Re2–Cl6	104.0(2)	Rh2–Rh1–O2	86.1(6)
Cl5–Re2–Cl5′	152.2(5)	Rh2–Rh1–O4	83.4(9)
Re2–Re3–Cl7	102.9(2)	Rh2–Rh1–N4	95.0(8)
Cl7–Re3–Cl7′	154.0(5)	Rh2–Rh1–N6	174.0(9)
Cl7–Re3–Cl8	87 0(4)	Rh1–Rh2–O1	87.0(6)
Cl7–Re3–Cl8′	86.8(4)	Rh1–Rh2–N2	98.3(9)
Cl8–Re3–Cl8′	152 3(5)	Rh1–Rh2–N3	174.0(8)
Re5–Re4–Cl11	101.8(4)	Rh2–N1–C5	170(4)
Re5–Re4–Cl14	103.0(3)	Rh4–Rh3–O6	83.6(6)
Cl11–Re4–Cl12	85.5(5)	Rh4–Rh3–O7	84.6(6)
Cl12–Re4–Cl14	154.4(5)	Rh4–Rh3–N11	96.4(7)
Re5A–Re4A–Cl15	107.0(2)	Rh4–Rh3–N12	173.6(9)
Cl9–Re4A–Cl10	87.2(5)	O6–Rh3–N10	178(1)
Re4–Re5–Cl9	101.5(3)	Rh3–Rh4–O5	86.2(7)
Re4–Re5–Cl10	103.0(3)	Rh3–Rh4–N7	99.3(9)
Cl9–Re5–Cl10	87.1(4)	Rh3–Rh4–N9	172.8(8)

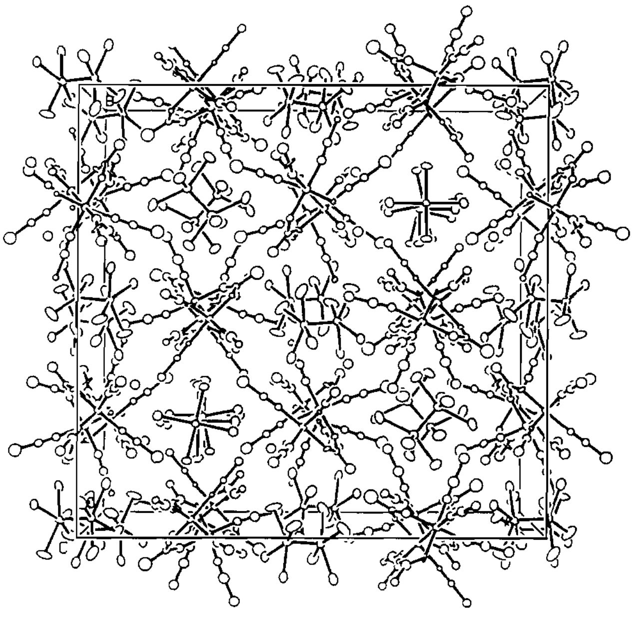

Fig. 2. An ORTEP unit cell packing diagram of $[Rh_2(OAc)_2(MeCN)_6][Re_2Cl_8]$ viewed down the *b* axis.

In addition to the fully occupied anion on a general position, there are two other locations in the lattice where anions reside. One octachlorodirhenate anion lies along a crystallographic C_2 axis and another $[Re_2Cl_8]^{2-}$ is perpendicularly bisected by a C_2 axis. As far as we are aware, the present structure is the only one in which an $[Re_2X_8]^{2-}$ unit is present in the same asymmetric unit with three different environments

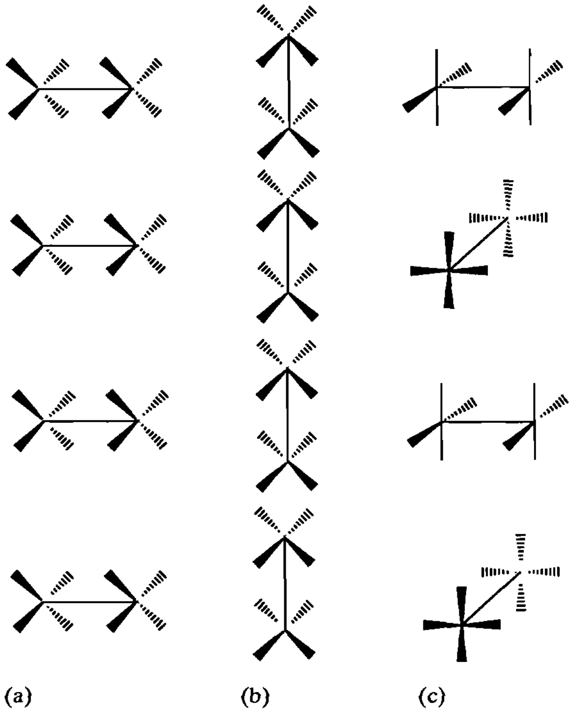

Fig. 3. Schematics of the three different stacking arrangements of $[Re_2Cl_8]^{2-}$ found in **1**: (a) parallel units, (b) end-to-end, (c) perpendicular.

[1, 8]. A comparison of the Re–Re separations in the three different anions is therefore in order; the values of 2.225(4) for Re1–Re1′, 2.216(3) for Re2–Re3, and 2.215(4) for Re4–Re5 are at the lower end of the range of values for Re–Re bonds in $[Re_2Cl_8]^{2-}$ which vary from 2.46(8) Å for $[2,4,6\text{-}(CH_3)_3C_5H_2NH]_2Re_2Cl_8$ to 2.21(1) Å for $[(DMF)_2H]_2Re_2Cl_8$ [8].

Inspection of the unit cell packing diagram for **1** reveals the influence of cation shape on the packing of the three different types of $[Re_2Cl_8]^{2-}$ anions. One $[Re_2]^{2-}$ unit is involved in a parallel stacking of M–M units in a large channel bordered by acetate groups of the surrounding dirhodium cations (Fig. 3(a)). A second type of $[Re_2Cl_8]^{2-}$ unit stacks in an end-to-end fashion (Fig. 3(b)) in a four-point star-shaped channel in which the chlorides point between the MeCN ligands of the $[Rh_2]^{2+}$ cations and towards the Rh atoms. Finally a third unique $[Re_2Cl_8]^{2-}$ packs with perpendicularly aligned metal units (Fig. 3(c)) in a second, slightly smaller star-shaped channel. This anion is the only one in the structure to exhibit disorder of the metal unit. The minor orientation is present at an occupancy of 19% which is within the range reported for other examples [8].

Solution behavior of $[Rh_2(OAc)_2(MeCN)_6][Re_2Cl_8]$

The electronic spectrum of a dilute solution containing $[Rh_2(OAc)_2(MeCN)_6][BF_4]_2$ and $[n\text{-}Bu_4N][Re_2Cl_8]$ monitored over a period of several hours revealed characteristic features of the two individual intact chromophores; these eventually disappeared with concomitant appearance of a new feature at $\lambda_{max} = 610$ nm. The same feature appears when a suspension of **1** is allowed to slowly dissolve with reaction in MeCN. The IR spectra of **1** and the soluble species formed by dissolution of **1** are different, further supporting the formation of a thermodynamic decomposition product. The four band pattern in the $\nu(C{\equiv}N)$ region of $[Rh_2(OAc)_2(MeCN)_6][Re_2Cl_8]$ reduces to two bands after dissolving in MeCN, and the ν(Re–Cl) stretch for **1** at 338 cm^{-1} is replaced by a feature at 350 cm^{-1} with a shoulder at 320 cm^{-1}.

Numerous efforts to elucidate the identity of the product (or products) resulting from the dissolution of **1** met with limited success. We reasoned that one of two processes could be occurring to destroy $[Rh_2(OAc)_2(MeCN)_6][Re_2Cl_8]$ in solution; we hypothesized that either $[Re_2Cl_8]^{2-}$ eventually undergoes decomposition in MeCN, or that $[Rh_2(OAc)_2(MeCN)_6]^{2+}$ abstracts chloride from $[Re_2Cl_8]^{2-}$. To test the first hypothesis, a sample of $[n\text{-}Bu_4N]_2[Re_2Cl_8]$ was dissolved in MeCN and stirred for one week after which time the electronic spectrum was measured; no sign of decomposition was detected as judged by the unchanged nature of the visible spectrum which showed the expected $\delta \rightarrow \delta^*$ transition ($\lambda_{max} = 680$ nm). The possibility of ligand redistribution was tested by reacting $[Rh_2(OAc)_2(MeCN)_6][BF_4]_2$ with two equivalents of ppnCl. This chemistry did not proceed cleanly, nevertheless we noted that the mixture did not display properties similar to those of the thermodynamic product(s). We can, therefore, conclude that simple ligand exchange is not responsible for the degradation of the two dinuclear complexes in solution. The possibility that the two charged species are undergoing reaction with each other to give a neutral mixed-metal compound is under investigation.

Supplementary material

Full tables of crystal parameters, bond distances, bond angles, anisotropic displacement parameters and tables of observed and calculated structure factors are available upon request from author K.R.D.

Acknowledgements

We thank Drs J. Eglin, C. James and L. Daniels for their help with data collection and D. Ward for assistance with the ORTEP program. We also thank Johnson Matthey for a loan of $RhCl_3 \cdot xH_2O$ and the National

Science Foundation (CHE-8914915) and the Michigan State University Center for Fundamental Materials Research for financial support.

References

1 F.A. Cotton, A.C. Price, R.C. Torralba and K. Vidyasagar, *Inorg Chim. Acta, 175* (1990) 281.

2 S.N. Bernstein and K.R. Dunbar, *Angew. Chem., Int. Ed Engl, 31* (1993) 1360.

3 W. Clegg, G. Pimblett and C.D. Garner, *Polyhedron 5,* (1986) 31.

4 T.J. Barder and R.A. Walton, *Inorg Synth, 23* (1986) 116.

5 G.M. Sheldrick, *SHELXS-86,* program for the solution of crystal structures, University of Gottingen, Germany, 1986.

6 P T. Beurskens, *DIRDIF: Direct Methods for Difference Structures,* an automatic procedure for phase extension and refinement of difference structure factors. *Tech Rep 1984/1,* Crystallography Laboratory, Toernooiveld, 6525, Ed Nijmegen, Netherlands, 1984.

7 G. Pimblett, C.D. Garner and W. Clegg, *J. Chem Soc., Dalton Trans.,* (1986) 1257.

8 F.A. Cotton and R.A. Walton, *Multiple Bonds Between Metal Atoms,* Clarendon, Oxford, 1993.